Ilkogretim Online - Elementary Education Online, Year; Vol 20 (Issue 4): pp. 1147-1155
http://ilkogretim-online.org
doi: 10.17051/ilkonline.2021.04.128

Design and Fabrication of Slot Loaded 1x2 Array Antennas for Multi-band Application

Gazala Pravin, Department of Physics & Electronics, Barkatullah University, Bhopal, India, g.rinkykhan@gmail.com
Alok Kumar Rastogi, Institute for Excellence in Higher Education, Bhopal, India

Abstract- In this article, an analysis of 1×2 array antenna has been presented for multiband applications that is etched on FR-4 substrate ($\tan(\delta) = 0.02, \varepsilon_r = 4.3$). This structure contains two rectangular-shaped radiating element, ground plane and feed lines. The position of resonance frequencies ($f_{TM\,10}, f_{TM\,02}, f_{TM\,12}, f_{TM\,20}$) are revised by the length of vertical and horizontal arms of the L and T-shaped slot. The proposed antenna exhibits resonances at frequencies 2.18 (2.16-2.2 GHz with bandwidth 1.83%), 3.22 (3.2-3.24 GHz with bandwidth 1.24%), 4.32 (4.3-4.34 GHz with bandwidth 0.93%) and 4.56 (4.54-4.58 GHz with bandwidth 0.87%) GHz. The series of equations have been deduced after studying the surface current distribution at resonating frequencies. Deformation of radiation pattern in both principal plans has been observed at frequencies 4.32 and 4.56 GHz.

Keywords: - Mode, Surface current distribution, Resonance frequency, Radiation pattern, Array antenna.

I. INTRODUCTION

Need of small antennas are increasing in modern communication system day by day. The printed antennas are potential candidate for wireless technology because of their physical structure. A part from above property they also offer some other merits like facile fabrication, small cost, easy integration with microwave circuit and ability to produce circular and electrical polarization [1]-[5]. Discontinuities play a prominent role in printed antenna which can be truncated on radiating edge or non radiating edge of the patch. These discontinuities can be also embedded in ground plane or mid surface of the radiating element. Slots or discontinuities alter the position of resonant frequency ($f_o = c/L\sqrt{\varepsilon_r}$) of resonating modes (fundamental modeTM_{10}, orthogonal mode TM_{01} or higher order modes $TM_{11}, TM_{12}, TM_{21}$) by changing the path of the length of the current vectors. Slot also affects the phase velocity ($V_p = 1/\sqrt{LC}$) of resonating modes by changing the value of inductance (L) and capacitance (C) of the antenna [6]-[10]. Several applications like sonar, satellite communication radar etc requires high gained antenna [11] & [12]. The high gain of the antenna depends on the no of elements, their geometry and arrangement of the elements [13]-[15]. By using parasitic element [16] & [17], photonic band gap structure [18], high permittivity substrate the gain of the antenna can be enhanced [19].

In this communication, we have designed used 1x2 array antenna for multiband operation which is fabricated on FR-4 substrate. The effect of lengths of the slot L and T shaped has been investigated on fundamental modeTM_{10}, orthogonal mode TM_{02} and higher order modes TM_{12}, TM_{22}. The experimental results exhibits that the proposed antenna is resonating at frequencies 2.18, 3.22, 4.32 and 4.56 GHz. The series of equations have been deduced after studying the surface current distribution at resonating frequencies. The detail of the proposed antenna has been given below.

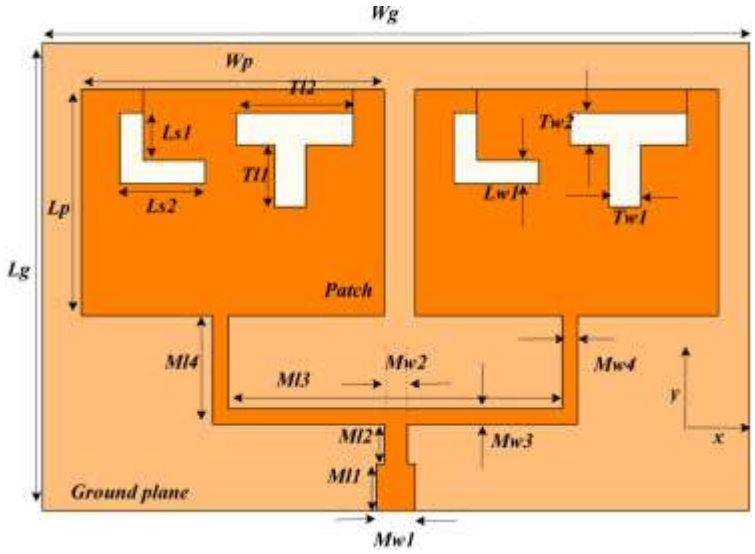

Figure 1. Optimized geometry of proposed 1x2 array antenna.

Table 1. Parameters and optimized dimension of proposed 1x2 array antenna.

Parameter	Dimension (mm)	Parameter	Dimension (mm)	Parameter	Dimension (mm)	Parameter	Dimension (mm)
W_p	39	L_g	61	$Ml1$	6	$Tl2$	15
L_p	29	$\hbar$	1.6	$Ml2$	5	$Mw3$	2
$Ls1$	6	$Tw2$	4	$Ml3$	43	$Tl1$	8
$Ls2$	11	W_g	90	$Ml4$	14	$Mw4$	2
$Lw1$	3	$Tw1$	4	$Mw1$	5	$Mw2$	3

II. ANTENNA CONFIGURATION

The optimized geometry of 1×2 arrays antenna has been depicted in figure 1 which is printed on FR-4 substrate with the permittivity ($\mathcal{E}$) of 4.3, tangent loss (tanδ) 0.02 and height (h) 1.6 mm. The parameters and optimized dimensions of the proposed antenna have been listed on table 1. This structure has been placed on azimuthal plane and Z-axis is normal to the radiating structure. L and T slots are truncated near to the top radiating edge of the each element. These slots basically modify the position of resonance frequencies of the modes. The length of vertical arms of these slots affects

the resonance frequency of higher order modes while horizontal arms affect the position of resonance frequency of fundamental mode and their harmonics. On bottom radiating edge of the each element is integrated with Microstrip feed line which delivers the electromagnetic energy to the elements. The characteristic impedance of the feed line depends on the width of feed which is calculated by equation (1).

$$Z_0 = \frac{\eta}{2\pi\sqrt{\varepsilon_{reff}}} \ln\left\{\frac{8\hbar}{w} + \frac{0.25w}{\hbar}\right\} \quad (1)$$

Where η and w are intrinsic impedance of the free space and width of the feed line respectively. On bottom side of the dielectric, rectangular shaped ground plane ($L_g \times W_g$) has been printed The dimension of the each element ($L_p \times W_p$) has been calculated from below equation and these elements are designed for resonant frequency $f_0 = 2.4\ GHz$. The width of the single element has been determined by equation (2).

$$W_p = \frac{C}{2f_0\sqrt{(\varepsilon_r + 1)/2}} \quad (2)$$

The fringing fields are responsible for radiation from printed antenna. Due to these fields the electrical length of the patch has increased which is larger than the physical length of the antenna. The effective dielectric constant and extension in length can be determined by following equations (3) and (4).

$$\varepsilon_{reff} = \frac{\varepsilon_r + 1}{2} + \frac{\varepsilon_r - 1}{2}[1 + 12\frac{W_p}{h}]^{-0.5} \quad (3)$$

$$\frac{\triangle L}{h} = \frac{0.412(\varepsilon_{reff} + 0.3)\left(\frac{W_p}{h} + 0.264\right)}{(\varepsilon_{reff} - 0.258)\left(\frac{W_p}{h} + 0.8\right)} \quad (4)$$

The physical length of the patch can be determined by following equations (5) and (6).

$$L_e = \frac{C}{2f_0\sqrt{\varepsilon_{reff}}} \quad (5)$$

$$L_p = L_e - 2 \triangle L \quad (6)$$

III. Development of 1x2 Array antennas

Evolution of the 1x2 array antenna and comparison of S_{11} characteristics have been depicted in figure 3. Antenna 1 contains feed structure and two rectangular shaped radiating elements which are designed for frequency 2.4 GHz. After feeding the electromagnetic energy, the fundamental mode (TM_{10}), harmonics of fundamental mode (TM_{20}), second harmonic of orthogonal mode (TM_{02}) and other higher order modes (TM_{20}, TM_{22}) are excited. The simulated resonance frequencies of $TM_{10}, TM_{02}, TM_{12}, TM_{20}$ and TM_{22} modes are 2.35, 3.6, 4.42, 4.61 and 5.8 GHz respectively. The difference ($E(\%) = 100 * (f_{calculated} - f_{simulated})/f_{calculated}$) between simulated and calculated resonance frequencies has been also found. Table 2 exhibits an error between simulated and calculated resonance frequencies.

Table 2. Error between calculated and simulated resonance frequencies..

Mode	$f_{calculated}$ (GHz)	$f_{simulated}$ (GHz)	$\lvert E(\%)\rvert$
TM_{10}	2.36	2.35	0.42
TM_{02}	3.54	3.6	1.69
TM_{12}	4.26	4.42	3.75
TM_{20}	4.72	4.61	2.33
TM_{22}	5.9	5.8	1.69

IV. Results and Discussion

a) S_{11} Characteristic and Input impedance

Prototype of 1x2 array antenna has been depicted in figure 2. The proposed antenna is numerically analyzed by CST Microwave studio and Sonnet. The experimental results (S_{11} characteristic and input impedance) are measured through VNA N9923A in frequency band 2 to 6 GHz. The fabricated antenna is resonating at four frequencies 2.22, 3.34, 4.5 and 4.76 GHz and covers three frequencies band 2.2-2.22 GHz with bandwidth 0.9%, 3.3-3.36 GHz with bandwidth 1.8% and 4.44-4.8 GHz with bandwidth 7.8%. Table 3 represents the measured and simulated return loss at resonating frequencies. An error between measured and simulated has been found because of fabrication error and variation of dielectric constant. Figure 3 represents the locus of input impedance (measured) of the proposed antenna. Loops have been found in smith chart due to coupling between modes.

Table 3. Measured and simulated resonating frequency.

Sonnet		CST		Measured	
Frequency (GHz)	Return loss (dB)	Frequency (GHz)	Return loss (dB)	Frequency (GHz)	Return loss (dB)
2.18	-8.33	2.18	-11.61	2.22	-12.84
3.24	-45.23	3.22	-20.399	3.34	-17.29
4.36	-21.13	4.32	-19.86	4.5	-11.83
4.56	-17.76	4.56	-17.994	4.72	-17.83

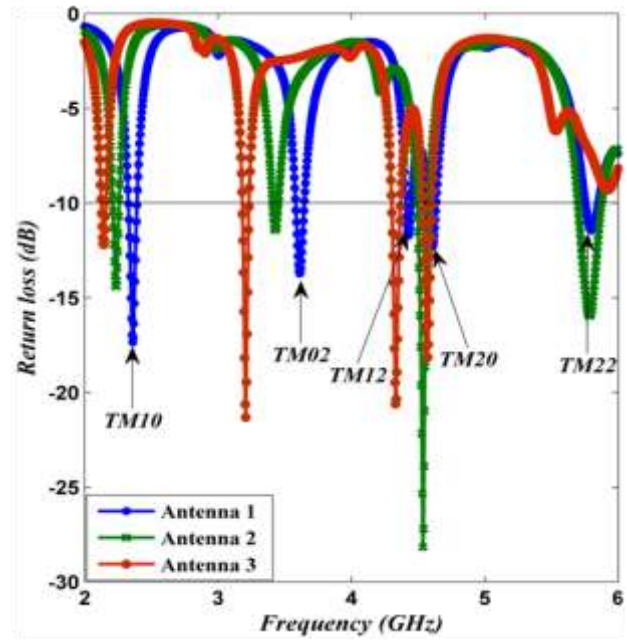

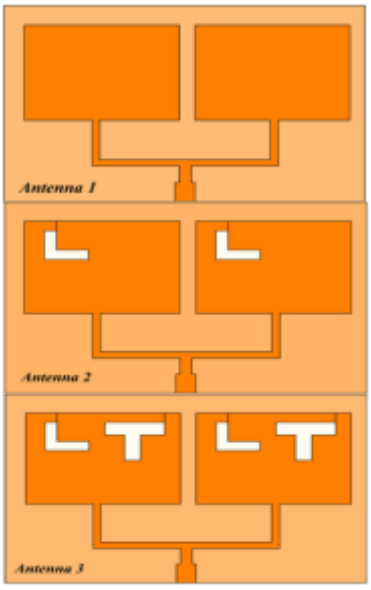

Figure 2. Evolution of the proposed antenna and comparison of S_{11} Characteristic of antenna1, 2 and 3.

b) Surface current distribution

The vector current distributions have been depicted in figure 5 at each resonating frequency. At f_1 2.18 GHz, The current vectors are distributed along the length of the patch which is similar to TM_{10} mode. It

can be also noticed that current density is maximum around L and T shaped slot. The horizontal arm of L and T shaped slots are perpendicular the current vectors which are distributed along the length. Horizontal arm of the both slots increases the patch length of current vectors. The resonance frequency f_1 can be determined by following equations
(7) and (8).

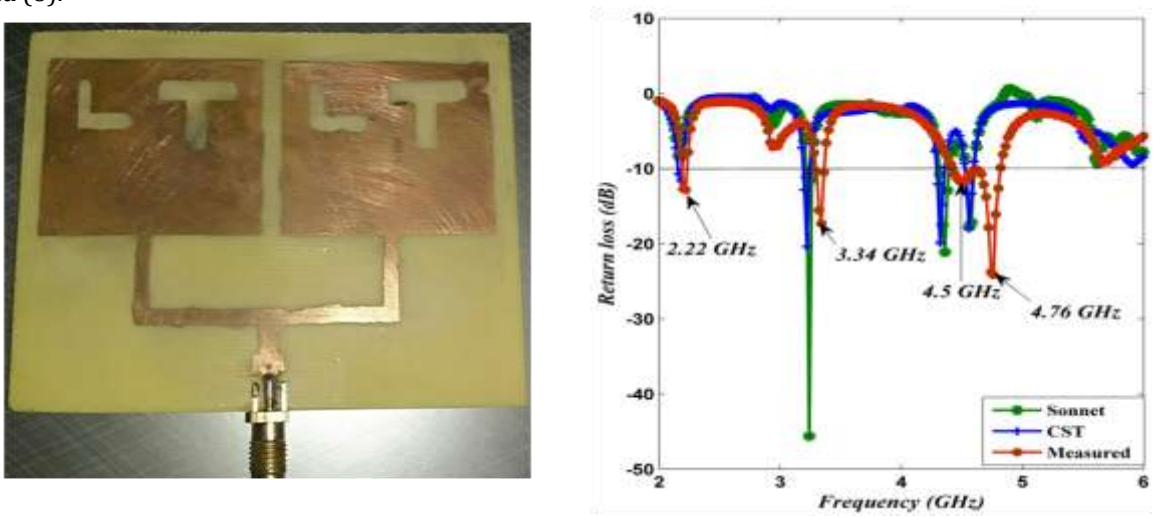

Figure 3. Fabricated antenna and comparison of measured and simulated S_{11} characteristics

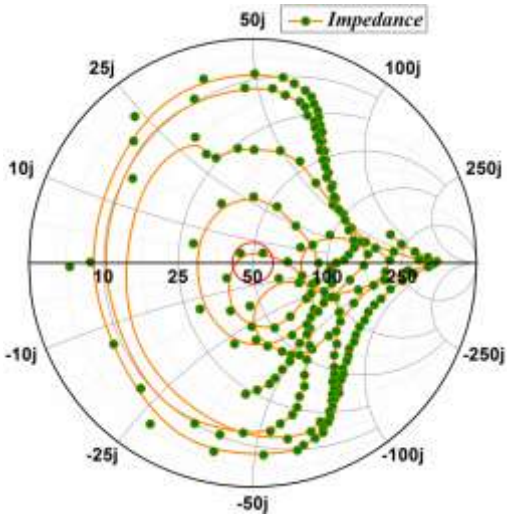

Figure 4 Measured input impedance of the proposed antenna.

$$l = L_p + L_{s2}/2 \tag{7}$$

$$f_1 = \frac{c}{2 * l * \sqrt{\varepsilon_r}} \tag{8}$$

The calculated value of f_1 is 2.1 GHz which is nearly equal to 2.18 GHz. An error (3.66%) between simulated and calculated has been found and can be estimated by below equation (9).

$$e(\%) = \frac{f_{simulated} - f_{calculated}}{f_{simulated}} * 100 \quad (9)$$

At f_2 3.22 GHz, current intensity is maximum around the slot as well as two half wave variation of current vectors have been investigated which is similar to TM_{02} mode. Vertical arm of the both slots affect the current distribution. The resonance frequency f_2 can be determined by following equations (10) and (11).

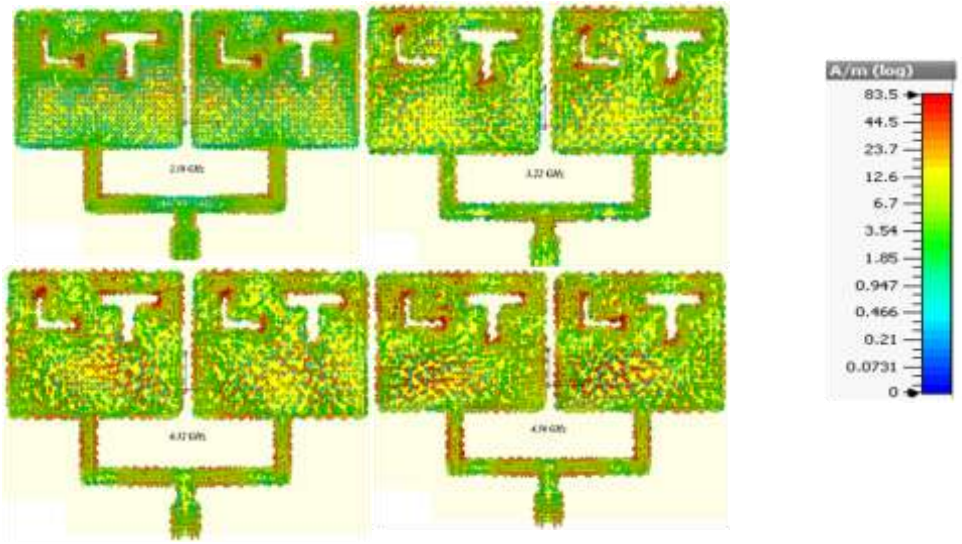

Figure 5. Current distribution at resonating frequencies

$$l_1 = W_p + (T_{l1} + T_{w2})/2 \quad (10)$$

$$f_2 = \frac{c}{l_1 * \sqrt{\varepsilon_r}} \quad (11)$$

The calculated value of f_2 is 3.2 GHz which is nearly equal to 3.22 GHz. An error (0.6%) between simulated and calculated has been found and can be estimated by below equation (12).

$$e_1(\%) = \frac{f_{simulated} - f_{calculated}}{f_{simulated}} * 100 \quad (12)$$

At f_3 4.32 GHz, current distribution is similar to TM_{12} mode. This mode is affect by both arms of the slots. It has been inspected that the current is maximum around the slots. At f_4 4.56 GHz, the current vectors are distributed along the length of the patch which is similar to TM_{20} mode. The horizontal arm of L and T shaped slots are perpendicular the current vectors which are distributed along the length. Horizontal arm of the both slots increases the patch length of current vectors. The resonance

frequency f_4 can be determined by following equations (13) and (14).

$$l_2 = L_p + L_{s2}/2 \quad (13)$$

$$f_4 = \frac{c}{l_2 * \sqrt{\varepsilon_r}} \tag{14}$$

The calculated value of f_4 is 4.2 GHz which is nearly equal to 4.56 GHz. An error (7.89%) between simulated and calculated has been found and can be estimated by below equation (15).

$$e_2(\%) = \frac{f_{simulated} - f_{calculated}}{f_{simulated}} * 100 \tag{15}$$

c) Radiation Pattern

The far field patterns of the proposed antenna have been displayed on figure 6. Far field patterns of this antenna are simulated in H-plane and E-plane with 10 degree increment at 2.18, 3.22, 4.32 and 4.56 GHz. It has been investigated that number of modes are increased as frequency increases. As shown in figure 6, the patterns are distorted in both planes which confirm that existence of higher order modes. The directionality of the E plane pattern has been reduced as frequency increases.

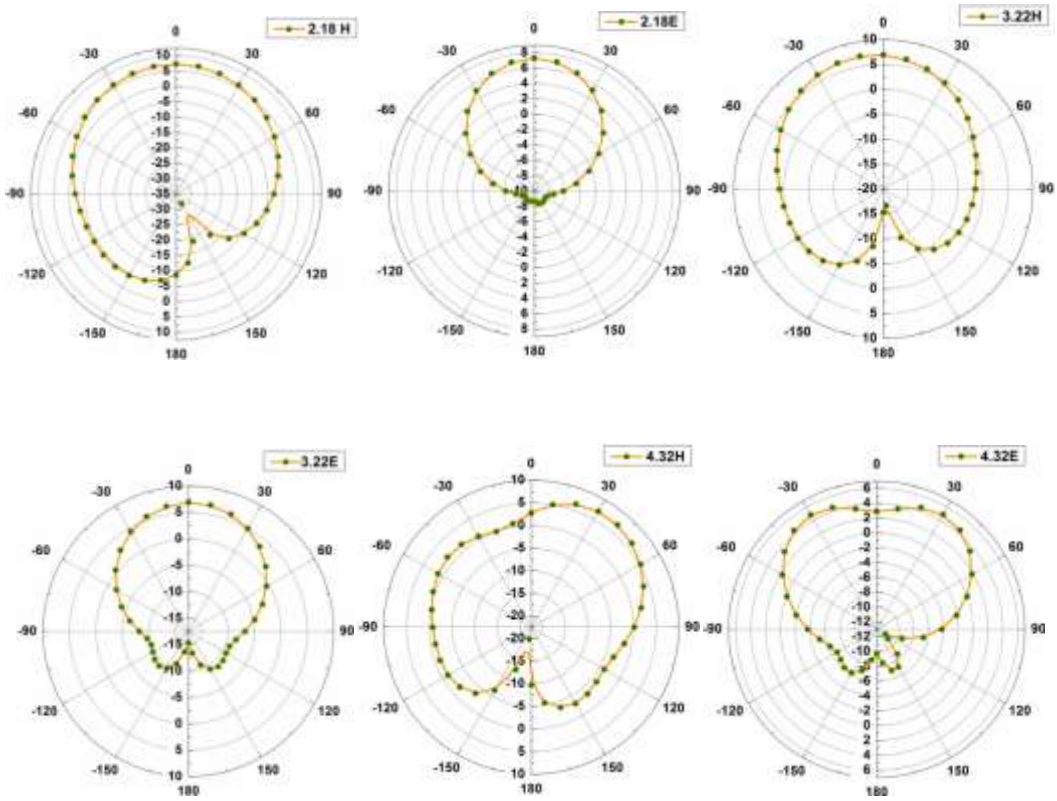

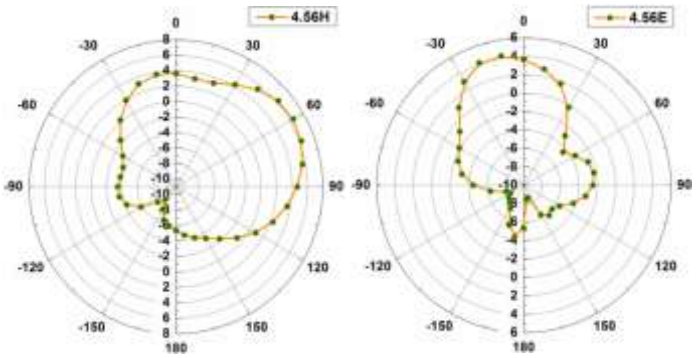

Figure 6. E plane and H plane pattern at resonating frequencies

V. CONCLUSION

An analysis of 1x2 array antenna has been designed and experimentally verified. This structure is resonating at four frequencies 2.18, 3.22, 4.32 and 4.56 GHz. It has been
also investigated that the vertical and horizontal arms of the L and T shaped slot affect the current distribution. Due to slot resonance frequency position of the fundamental mode and other higher order modes have been changed. The formulation of each resonating frequencies is also done. It has been noticed that the radiation pattern is distorted at higher frequencies.

REFERENCES:

[1] C.A. Balanis, "Antenna Theory Analysis, and Design", Textbook 3rd Edition. (2005), New Jeresey, N Wiley and Sons.

[2] B. Shukla, N. R. Kashyap, R. Baghel, "A broadband novel design of Scarecrow-shaped patch antenna for compact Broadband application" International journal of microwave and wireless technology,**10**(2018),351-359.

[3] Kamakshi and J. A. Ansari. A. Singh, and A. Mohammad "Desktop Shaped Broadband Microstrip Patch Antennas for Wireless Communications", Progress In Electromagnetics Research Letters, Vol. **50**(2014), 13–1.

[4] C. Oesteges, and B. Clerck, "MIMO Wireless Communication", ed. 1st Acad. press. (2007) 1-480.

[5] He-Xiu Xu, Wang Gua-Ming, Qi Mei Qing and Cai Tong, "Compact fractal left-handed structures for improved cross-polarization radiation pattern", IEEE Transctions Antenna Propagation, **62** (2014):546–554.

[6] A. A. Deshmukh and G. Kumar, "Compact broadband u-slot loaded rectangular microstrip antennas" microwave and optical technology letters , **46**(2005), 556-559.

[7] A. A. Deshmukh and R. P. Ray "Formulation of Resonance Frequencies for Dual-Band Slotted Rectangular Microstrip Antennas", IEEE Antennas and Propagation Magazine, **54**(2012), 78-97.

[8] A. A Deshmukh and K.P. Ray. "Analysis of Broadband Psi (Ψ)-Shaped Microstrip Antennas", IEEE Antennas and Propagation Magazine, **55**(2013), 107-123.

[9] A. A. Deshmukh and G. Kumar "Broadband compact V-slot loaded RMSAs", Electronics Letters 17th.,**42**(2006), 951-952.

[10] A. A. Alazza, F. J. Harackiewiez and H. R. Gorla, "Very compact open-slot antenna for wireless communication system", progress In Electromagnetics research Letters, **51**(2015), 73-78.

[11] A. Chatterjee, T. Mondal, D. G. Patanvariyaa, K. Prasad, and R. Jagannath "Fractal-based design and fabrication of low-sidelobe antenna array", International Journal of Electronics and Communications (AEÜ) **83**(2018) 549–55.

[12] S. Koziel, S. Ogurtsov, W. Zieniutycz, and L. Sorokosz, "Expedited design of microstrip antenna subarrays using surrogate-based opti-mization", IEEE Antenna Wireless Propagation Letter, 13 (2014),635–638.
[13] J. H. Lu, "Cylindrical-rectangular microstrip array with high-gain operation for ieee 802.11j mimo applications", Progress In Electromagnetics Research Letters, **23**(2011), 1-7.
[14] A. Dalli, L. Zenkouar and S. Bri, "Study of Circular Sector Patch Array Antenna with Two and Four Elements for C and X Band", European Journal of Scientific Research ISSN 1450-216X **81**(2012), 150-159.
[15] S. H. Yeung, L. A. Garcia, and S. T. Kumar, "Salazar-Palma M. Thin and Compact dual-band four-element broadside patch antenna arrays", IEEE Antenna Wireless Propagation Letter;**13**(2014):567–70.
[16] R. Q. Lee, and K. F. Lee, "Gain enhancement of microstrip antenna with overlaying parasitic directors", IET Electronic. Letter,**24**(1988),656-658,.
[17] Qu. Shi-Wei, He De-Jun, S. Yang, Nie Za. "Novel parasitic micro strip arrays for low-cost active phased array applications", IEEE Transctions Antennna Propagation;**62**(2014),1731–1737.
[18] J. S. Kuo and G. B. Hsieh, "Gain enhancement of a circularly polarized equilateral triangular microstrip antenna with a slotted ground plane", IEEE Transctions Antennas Propagation, **51**(2003),1652.
[19] C. S. Hong, "Small annular slot antenna with capacitor loading", IET Electronic Letter, **36**(2003),75-83.